

## THERMAL EXPANSION OF LIQUID CRYSTALLINE AMPHIPHILIC DI-BLOCK COPOLYMER OBSERVED BY SIMULTANEOUS DSC-XRD

R. Watanabe<sup>1</sup>, T. Iyoda<sup>1,4</sup>, T. Yamada<sup>2</sup> and H. Yoshida<sup>3,4\*</sup>

<sup>1</sup>Chemical Resources Laboratory, Tokyo Institute of Technology, 4259 Nagatsuta-cho, Midori-ku, Yokohama, Kanagawa 226-8503, Japan

<sup>2</sup>Graduate School of Engineering, Tokyo Metropolitan University, 1-1 Minamiosawa, Hachioji, Tokyo 192-0397, Japan

<sup>3</sup>Faculty of Urban Environment Science, Tokyo Metropolitan University, 1-1 Minamiosawa, Hachioji, Tokyo 192-0397, Japan

<sup>4</sup>JST-CREST, 4-1-8 Honmachi, Saitama 332-0012, Japan

Phase transition process of  $\text{PEO}_m$ -*b*-PMA(Az)<sub>n</sub> was investigated by the simultaneous DSC-XRD measurement using the synchrotron radiation facility. Four endothermic DSC peaks were observed during heating process. These DSC peaks were assigned to the melting of PEO, the transition from SmX, which is a mixture of super-cooled SmC and crystal, to SmC, from SmC to SmA, and from SmA to isotropic liquid state as determined by XRD profiles. In SmC phase, the liner expansion coefficient calculated from the spacing variation of the smectic layer distance was larger than that of the other phases. This result reflected the fact azobenzene moieties in the long-side chains of PMA(Az)<sub>n</sub> forming the smectic layers and then they were tilted and stood up during the heating process.

**Keywords:** amphiphilic di-block copolymer, azobenzene, DSC-XRD, liquid crystalline polymer, smectic phase, thermal expansion

### Introduction

The liquid crystalline polymers (LCPs) are classified two categories, main chain type and side chain type. The main chain type LCPs contain mesogenic moieties such as multiaromatic rings in main chain, and demonstrate high glass transition temperature and isotropic transition. Most of main chain type LCPs show the nematic phase. The thermotropic mesophase of the polyesters based on 2,7-phenanthrene dicarboxylic acid and diethylester and alkanediols was assumed as the smectic phase due to the intermolecular interaction between phenanthrene moieties [1–3]. On the other hand, most of side chain type LCPs are amorphous polymers accompanying with unclear liquid crystalline phase due to the steric hindrance of mesogenic moieties in side chain.

The nano-scale structures and phase transitions of a series of liquid crystalline type amphiphilic di-block copolymers,  $\text{PEO}_m$ -*b*-PMA(Az)<sub>n</sub>, is reported in order to handle these copolymers as nanomaterials [4–7]. These copolymers consist of polyethylene oxide,  $\text{PEO}_m$ , as a hydrophilic block, and the comb-shaped polymers of polymethacrylate with azobenzene, PMA(Az)<sub>n</sub>, which is mesogenic moiety, as a hydrophobic block.  $\text{PEO}_m$ -*b*-PMA(Az)<sub>n</sub> provides two types of periodic nanostructures, that is, a nanophase-separated structure with hydrophilic cylinders and a liquid crystalline with lamellar structures in hydrophobic matrix.

For  $\text{PEO}_m$ -*b*-PMA(Az)<sub>n</sub>, the liquid crystalline structure existed in nano-scale spaces surrounding hydrophilic PEO cylinders and the molecular motion of PMA(Az)<sub>n</sub> chains having mesogenic groups in the side chain was restricted by bonding with  $\text{PEO}_m$  chains. According to our previous works [5, 7], the orientations of mesogenic groups in liquid crystal phase in the hydrophobic matrix affect the orientation of PEO cylinders. The phase transition behaviour of liquid crystal in the nanophase-separated structure is interested from thermodynamic and structural viewpoints. In this study, the thermal expansion of the smectic layer was investigated by the simultaneous DSC-XRD measurement in order to characterize liquid crystalline phases.

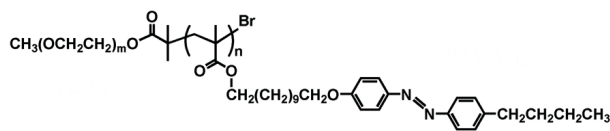
### Experimental

A series of liquid crystalline type amphiphilic di-block copolymers, poly(ethylene oxide)-*b*-poly[11-[4-(4-butylphenylazo)phenoxy]undecyl methacrylate],  $\text{PEO}_m$ -*b*-PMA(Az)<sub>n</sub>, (Scheme 1), are synthesized by the atom transfer radical polymerization [4, 6]. The degrees of polymerization of block sequences, which are shown as *m* for PEO and *n* for PMA(Az), were determined by <sup>1</sup>H-NMR. Three types of PEO length, *m*=40, 114, and 454, were used for the hydrophilic part of di-block copolymers. Two kinds of PMA(Az)<sub>n</sub>

\* Author for correspondence: ryokow-st@res.titech.ac.jp

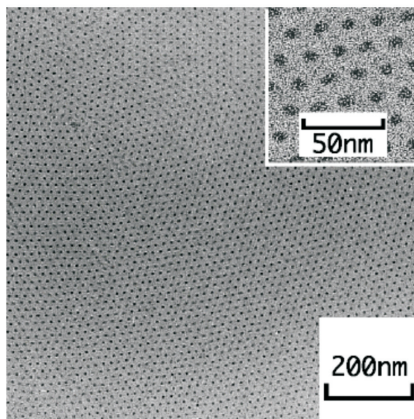
**Table 1** Linear thermal expansion coefficients  $\alpha$ [K $^{-1}$ ] at various temperatures

	Slope 1	Slope 2	Slope 3	Slope 4
PEO <sub>40</sub> - <i>b</i> -PMA(Az) <sub>92</sub>	1.5·10 $^{-3}$	6.6·10 $^{-3}$		8.1·10 $^{-4}$
PEO <sub>114</sub> - <i>b</i> -PMA(Az) <sub>10</sub>		7.1·10 $^{-3}$		
PEO <sub>114</sub> - <i>b</i> -PMA(Az) <sub>20</sub>	2.9·10 $^{-3}$	3.0·10 $^{-3}$	6.8·10 $^{-3}$	
PEO <sub>114</sub> - <i>b</i> -PMA(Az) <sub>45</sub>	3.8·10 $^{-4}$	1.4·10 $^{-3}$	7.2·10 $^{-3}$	3.9·10 $^{-4}$
PEO <sub>114</sub> - <i>b</i> -PMA(Az) <sub>55</sub>	1.3·10 $^{-3}$	3.3·10 $^{-3}$	7.9·10 $^{-3}$	3.5·10 $^{-4}$
PEO <sub>454</sub> - <i>b</i> -PMA(Az) <sub>35</sub>	2.4·10 $^{-3}$	2.4·10 $^{-3}$	7.5·10 $^{-3}$	7.0·10 $^{-4}$
PEO <sub>454</sub> - <i>b</i> -PMA(Az) <sub>90</sub>	4.1·10 $^{-4}$	2.9·10 $^{-3}$	7.5·10 $^{-3}$	8.4·10 $^{-4}$
PMA(Az) <sub>20</sub>		3.1·10 $^{-3}$	7.0·10 $^{-3}$	
PMA(Az) <sub>60</sub>	<10 $^{-5}$	3.6·10 $^{-3}$	8.4·10 $^{-3}$	1.2·10 $^{-3}$
Phase	SmX	SmC	transition SmC	SmA

**Scheme 1** The liquid crystalline di-block copolymer, PEO<sub>m</sub>-*b*-PMA(Az)<sub>n</sub>, consisting of polyethylene oxide block and polymethacrylate block with azobenzene moiety

prepared by the atom transfer radical polymerization were used as a side chain type liquid crystalline homopolymer. Samples used through this study were listed in Table 1.

The simultaneous DSC-XRD measurements were carried out at beam line 10C, Photon Factory, High Energy Accelerator Research Organization, Tsukuba, Japan. The wavelength of monochromatic X-ray for DSC-XRD was 0.1488 nm. The scattering X-ray was detected by a one-dimensional position sensitive proportional counter (PSPC, 512 channels, Rigaku Co. Ltd.). The distance between samples and PSPC was 550 mm, which covered

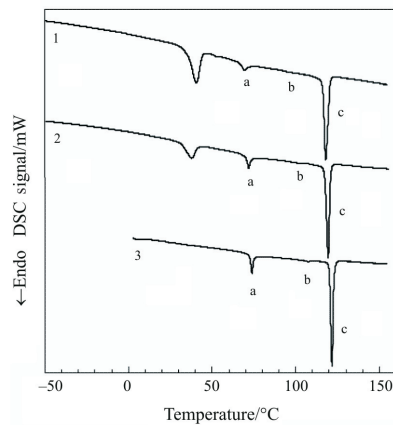
**Fig. 1** TEM micrograph of PEO<sub>114</sub>-*b*-PMA(Az)<sub>45</sub> annealed at 140 degrees for 24 h. The PEO microdomains appear darker due to staining with RuO<sub>4</sub>

1.02 nm $s^{-1}$ =(2πq) $^{-1}$ =(2sinθ/λ) $^{-1}$ <60.8 nm. The simultaneous DSC [8] was set on the small X-ray scattering optics. The heating rate of DSC was 5 K min $^{-1}$  and XRD profiles were stored each 2.5 K. The temperature and enthalpy were calibrated by pure indium and tin. The samples were hand-pressed to form pellets and sandwiched with two thin aluminum foils and crimped in an aluminum sample vessel [8]. The sampling mass used was about 5 mg.

DSC measurement was carried out by a Seiko Instruments DSC 6200 equipped with a cooling apparatus at 5 K min $^{-1}$  under a dry nitrogen atmosphere.

## Results and discussions

Figure 1 shows a typical transmission electron micrograph of PEO<sub>114</sub>-*b*-PMA(Az)<sub>45</sub>, the sample was annealed at 140°C for 24 h to establish the equilibrium nano-scale structure. Cylindrical PEO micro-domains shown as black spots were hexagonally packed in the PMA(Az) matrix where the smectic layers of long-side

**Fig. 2** DSC heating curves of 1 – PEO<sub>114</sub>-*b*-PMA(Az)<sub>45</sub>, 2 – PEO<sub>114</sub>-*b*-PMA(Az)<sub>100</sub> and 3 – PMA(Az)<sub>60</sub> at 5 K min $^{-1}$

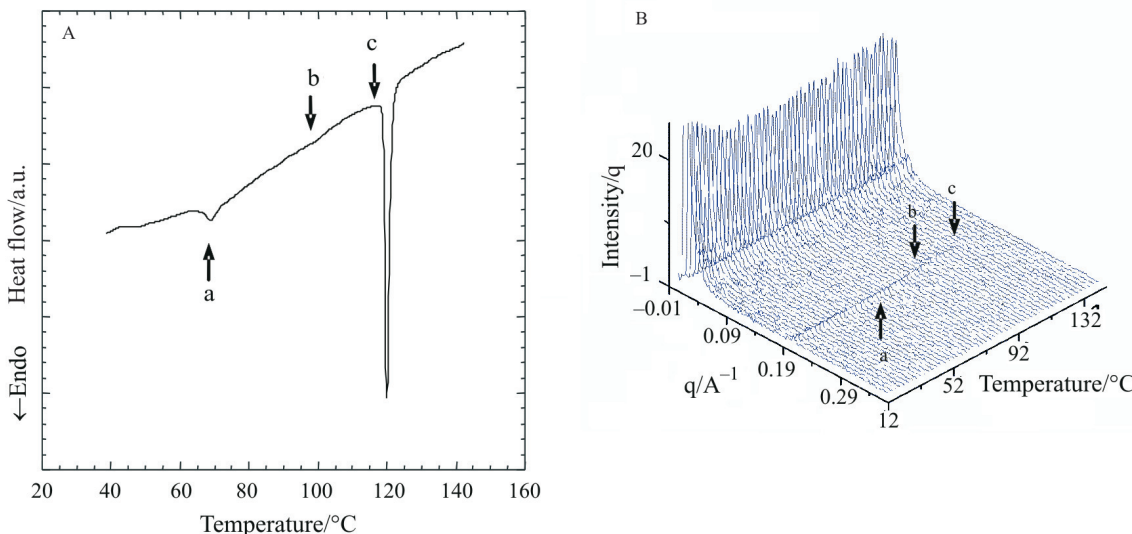


**Fig. 3** DSC curve (A) and stacked XRD profiles (B) of  $\text{PEO}_{114}\text{-}b\text{-PMA(Az)}_{45}$  observed by the simultaneous DSC-XRD on heating at  $5 \text{ K min}^{-1}$

chains containing azobenzene moieties were formed. These structures were confirmed by XRD measurement [4–6].

DSC heating curves of  $\text{PEO}_{114}\text{-}b\text{-PMA(Az)}_{45}$ ,  $\text{PEO}_{114}\text{-}b\text{-PMA(Az)}_{100}$  and  $\text{PMA(Az)}_{60}$  are shown in Fig. 2. Block copolymers showed four endothermic transitions, the transition at  $30^\circ\text{C}$  was the melting of PEO domains and the other transitions corresponded to  $\text{PMA(Az)}_n$  domains. DSC curve of  $\text{PMA(Az)}_{60}$  showed three transitions which indicated as *a*, *b* and *c*. All these transitions were thermo reversible transitions accompanying with small degree of super-cooling comparing with the melting of PEO. The temperature of transition *a* depended slightly on the sequence length, *n* of  $\text{PMA(Az)}_n$ , and the block copolymers showed slightly lower temperature of transition *a* than that of homopolymers. However the transition enthalpy per one repeating unit was almost the same ( $2.8 \text{ kJ mol}^{-1}$ ). The temperature of transition *c* depended strongly on *n* of  $\text{PMA(Az)}_n$  for both homopolymer and block copolymers, however the transition entropy per one repeating unit was almost the same ( $37 \text{ J K}^{-1} \text{ mol}^{-1}$ ). As the transition *b* was broad and weak, the evaluation of transition enthalpy was difficult.

DSC curve and XRD profiles of  $\text{PEO}_{114}\text{-}b\text{-PMA(Az)}_{45}$  obtained by the simultaneous DSC-XRD measurement on heating are shown in Fig. 3A and B, respectively. Three transitions were observed on DSC curve at around 65 (*a*), 99 (*b*), 115 (*c*)  $^\circ\text{C}$  without the melting of PEO sequence. Through the heating process, a single XRD scattering peak was observed at around  $0.2 \text{ Å}^{-1}$  (Fig. 3B). This peak corresponded to the smectic layer spacing of side-chains containing azobenzene moieties in consistency with

its molecular length (c.a. 3 nm) assuming *trans* conformations of both alkyl chain and azobenzene. The textures corresponding to smectic phases were observed by the polarized optical microscopy observation [1]. As the XRD scattering peak disappeared above the transition *c* at  $115^\circ\text{C}$ , the transition *c* was assigned as the isotropic transition of the smectic phase to the isotropic liquid phase. The isotropic transition entropy per one repeating unit was  $37 \text{ J K}^{-1} \text{ mol}^{-1}$ , which was similar to the isotropic transition entropy of liquid crystals, such as  $3\text{--}13 \text{ J K}^{-1} \text{ mol}^{-1}$  for the smectic A – isotropic transition and  $10\text{--}43 \text{ J K}^{-1} \text{ mol}^{-1}$  for the smectic C – isotropic transition [9–12].

As indicated in Fig. 3B, the XRD scattering peak slightly shifted to the lower *q* upon heating. The temperature dependency of the smectic layer spacing, *d*<sub>s</sub>

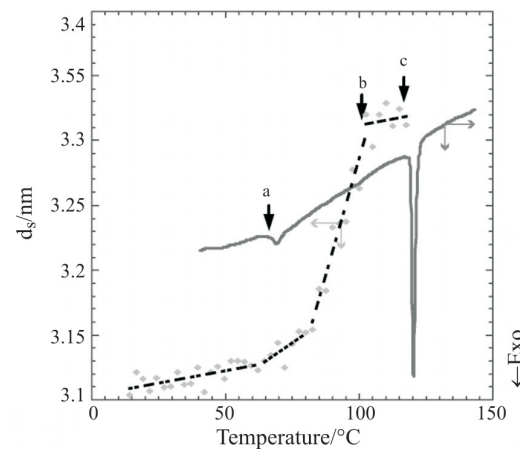


**Fig. 4** Temperature dependency of smectic layer spacing for  $\text{PEO}_{114}\text{-}b\text{-PMA(Az)}_{45}$ . ··· for slope 1, ··· for slope 2, ····· for slope 3, and — for slope 4

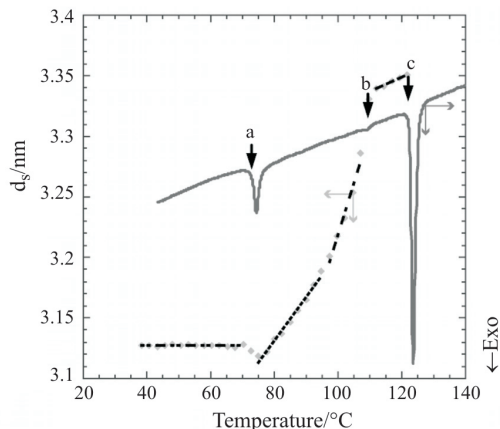


**Fig. 5** Temperature dependency of smectic layer spacing for PMA(Az)<sub>60</sub>. ··· for slope 1, ··· for slope 2, -·- for slope 3, and — for slope 4

for PEO<sub>114</sub>-*b*-PMA(Az)<sub>45</sub> and PMA(Az)<sub>60</sub> observed by DSC-XRD are shown in Figs 4 and 5. The  $d_s$  changes shown in Figs 4 and 5 divided to four regions, such as the first region below the transition *a* (slope 1), the second and third regions between the transitions *a* and *b* (slope 2 and slope 3), and the fourth region between the transitions *b* and *c* (slope 4). The thermal expansion coefficients ( $\alpha$  [K<sup>-1</sup>]) of smectic layer evaluated for each region for PEO<sub>114</sub>-*b*-PMA(Az)<sub>45</sub> were  $3.8 \cdot 10^{-4}$  (slope 1),  $1.4 \cdot 10^{-3}$  (slope 2),  $7.2 \cdot 10^{-3}$  (slope 3), and  $3.9 \cdot 10^{-4}$  K<sup>-1</sup> (slope 4), respectively. Thermal expansion coefficients in volume are  $8.2 \cdot 10^{-4}$  K<sup>-1</sup> (the smectic A phase),  $1.0 \cdot 10^{-3}$  K<sup>-1</sup> (the smectic C phase) and  $7 \cdot 10^{-4}$  K<sup>-1</sup> (the smectic B phase) for *p*-azoxyanisole [13], and  $4.11 \cdot 10^{-4}$  K<sup>-1</sup> (the crystalline phase) for *n*-amyl 4-(4-*n*-dodecyloxybenzylidene-amino)cinnamate [14]. Similar results are obtained for 4'-methoxybenzylidene-4-butylaniline (MBBA) and chiral liquid crystals [15–17]. As the linear  $\alpha$  of smectic layer evaluated from DSC-XRD corresponded to the one-dimensional  $\alpha$  parallel to the covalent bonding, the linear  $\alpha$  in this study should be smaller than the volumetric  $\alpha$  which was average value parallel and perpendicular to the covalent bonds.

Between the transitions *a* and *b*, there are two linear expansion relationships, slope 2 and slope 3, indicating the mechanism of thermal expansion was not simple. The  $\alpha$  value ( $1.4 \cdot 10^{-3}$  K<sup>-1</sup>) at slope 2 was similar to the value of smectic phase. However, the  $\alpha$  value ( $7.2 \cdot 10^{-3}$  K<sup>-1</sup>) at slope 3 was larger than that of liquid or liquid crystalline phases. Thus, it is reasonable to assume the azobenzene moieties were tilted and formed the smectic C phase (SmC) in the phase between the transitions *a* and *b*, and stood up during heating. Since the azobenzene moieties stood up in the smectic layer, the layer spacing increased dramatically.

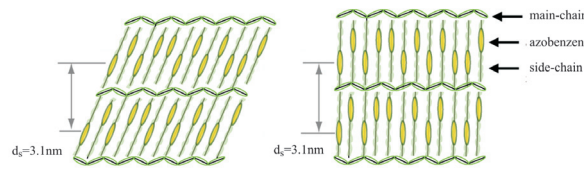


**Fig. 6** Possible schematic illustrations for the layer structures of the smectic liquid crystals, SmC and SmA, formed in PMA(Az)<sub>n</sub> block ( $d$  is the layer spacing)

When the temperature reached to the transition *b*, the azobenzene moieties were in the equilibrium state, and were aligned parallel to the smectic layer spacing. The linear  $\alpha$  value ( $3.9 \cdot 10^{-4}$  K<sup>-1</sup>) at slope 4, which was corresponded to that of the direction of covalent bond, was smaller than that of liquid crystalline phase and was similar to that of the crystalline state. The average layer spacing was 3.32 nm in the phase between the transitions *b* and *c* which was almost the same to the extended molecular length of side chain in PMA(Az), 3.3 nm, calculated by MM2 force field method. Therefore, the phase between the transitions *b* and *c* was assigned to the smectic A phase (SmA). Considering with the random conformation of main chains in the layer planes and the interaction of azobenzene moieties, the possible schematic model for the layer structures of the smectic phase formed in PMA(Az) block, where the long-side chains were regularly arranged forming a kind of interdigitated structure, was shown in Fig. 6.

In the phase below the transition *a*, the liner  $\alpha$  ( $3.8 \cdot 10^{-4}$  K<sup>-1</sup>) at slope 1 was almost the same with the liner  $\alpha$  ( $3.9 \cdot 10^{-4}$  K<sup>-1</sup>) at slope 4. The liner  $\alpha$  at slope 1 was in the range of the liner  $\alpha$  of the crystalline state of organic materials. Thus, the phase below the transition *a* was assigned as the crystalline state. However, the transition enthalpy of PEO<sub>m</sub>-*b*-PMA(Az)<sub>n</sub>, 2.8 kJ mol<sup>-1</sup>, was one-third of that of PMA(Az)<sub>n</sub> homopolymer, 8.7 kJ mol<sup>-1</sup>. These facts suggested that most of PMA(Az)<sub>n</sub> part of PEO<sub>m</sub>-*b*-PMA(Az)<sub>n</sub> was in the super-cooled smectic phase at temperature below the transition *a*. Therefore this phase was assigned to the smectic X phase (SmX), which indicated the mixing state with the crystal of PMA(Az) and the super-cooled SmC. In conclusion, the liquid crystalline state in PEO<sub>m</sub>-*b*-PMA(Az)<sub>n</sub> and PMA(Az)<sub>n</sub> changed from SmX, SmC, SmA and isotropic liquid at the transitions *a*, *b*, and *c*, respectively.

The linear  $\alpha$  of PEO<sub>m</sub>-*b*-PMA(Az)<sub>n</sub> and PMA(Az)<sub>n</sub> having different molecular mass were calculated in the same manner as described above, which were shown in Table 1. All PEO<sub>m</sub>-*b*-PMA(Az)<sub>n</sub> and PMA(Az)<sub>n</sub> showed the same tendency of temperature dependency of smectic layer spacing. Comparing PMA(Az)<sub>n</sub> homopolymers and PEO<sub>m</sub>-*b*-PMA(Az)<sub>n</sub>

copolymer, the liner  $\alpha$  at slope 1 of the homopolymers was smaller than that of copolymers due to the crystallinity difference. As the azobenzene moieties were packed tightly in the case of PMA(Az)<sub>n</sub> homopolymers, the restriction of thermal motion of azobenzene moieties gave the lower  $\alpha$  value than that of PEO<sub>m</sub>-*b*-PMA(Az)<sub>n</sub>. In SmA phase, the liner  $\alpha$  at slope 4 of PEO<sub>m</sub>-*b*-PMA(Az)<sub>n</sub> was slightly larger than that of PMA(Az) homopolymers. The XRD scattering peak from smectic layer of PEO<sub>m</sub>-*b*-PMA(Az)<sub>n</sub> was slightly broader than that of PMA(Az)<sub>n</sub> homopolymer. The order of SmA in PEO<sub>m</sub>-*b*-PMA(Az)<sub>n</sub> was slightly lower than that of PMA(Az)<sub>n</sub> homopolymer due to the restriction of PMA(Az)<sub>n</sub> which was connected with PEO sequence at the interface between the hydrophilic and hydrophobic domains as shown in Fig. 1. However, the values of liner  $\alpha$  at slope 2 and slope 3 of PEO<sub>m</sub>-*b*-PMA(Az)<sub>n</sub> were similar to those of PMA(Az)<sub>n</sub> homopolymers due to the molecular motion of azobenzene moieties.

## Conclusions

Thermal transition behaviors of PEO<sub>m</sub>-*b*-PMA(Az)<sub>n</sub> and PMA(Az)<sub>n</sub> were investigated by the simultaneous DSC-XRD method. PEO<sub>m</sub>-*b*-PMA(Az)<sub>n</sub> showed three endothermic DSC peaks corresponding to the phase changes of the PMA(Az)<sub>n</sub> domain during heating process. From the temperature dependency of the smectic layer spacing observed by DSC-XRD, the liner expansion coefficients ( $\alpha$  [K<sup>-1</sup>]) of the smectic layer spacing in each phase were calculated and characterized the liquid crystalline phases. The liquid crystalline states in this di-block copolymer were characterized

as SmX (mixture of crystal and super-cooled SmC), SmC and SmA in order of temperature increase.

## References

- 1 H. Yohsida, K. Masaka and S. Nakamura, Rept. Prog. Phys. Polym. Phys. Jpn., 41 (1998) 211.
- 2 H. Yoshida, Y. Houshito, K. Mashiko, K. Masaka and S. Nakamura, J. Therm. Anal. Cal., 64 (2001) 453.
- 3 H. Yoshida, M. Yang, K. Masaka, Y. Houshito, K. Mashiko and S. Nakamura, J. Therm. Anal. Cal., 70 (2002) 703.
- 4 Y. Q. Tian, K. Watanabe, X. Kong, J. Abe and T. Iyoda, Macromolecules, 35 (2002) 3739.
- 5 R. Watanabe, K. Watanabe, H. Yoshida and T. Iyoda, Polym. Preprints, Japan, 52 (2003) 2575.
- 6 K. Watanabe, Y. Q. Tian, H. Yoshida, S. Asaoka and T. Iyoda, Trans. Mater. Res. Soc. Japan, 28 (2003) 553.
- 7 H. Yoshida, K. Watanabe, R. Watanabe and T. Iyoda, Trans. Mater. Res. Soc. Japan, 29 (2004) 861.
- 8 H. Yoshida, R. Kinoshita and Y. Teramoto, Thermochim. Acta, 264 (1995) 173.
- 9 M. Sorai, 'Fundamental and Application of Calorimetry and Thermal Analysis' 3<sup>rd</sup> Edition, Ed. by JSCTA, p.149 (1994).
- 10 D. Marzotko and D. Demus, Pramana Suppl., 1 (1975) 189.
- 11 B. Bahadur, Mol. Cryst. Liq. Cryst., 35 (1976) 83.
- 12 D. Demus and R. Rurainski, Z. Phys. Chem., 253 (1973) 53.
- 13 M. Sorai and K. Saito, The Chemical Record, 3 (2003) 29.
- 14 K. Saito and M. Sorai, Ekisho, 5 (2001) 20.
- 15 E. Gulari and B. Chu, J. Chem. Phys., 62 (1975) 795.
- 16 E. McLaughlin, M. A. Shakespeare and A. R. Ubbelohde, Trans. Faraday Soc., 60 (1964) 25.
- 17 F. P. Price and J. H. Wendorff, J. Phys. Chem., 77 (1973) 2342.

DOI: 10.1007/s10973-005-7632-5